

Supporting Information

Redox-Activated Manganese-Based MR Contrast Agent

Galen S. Loving, Shreya Mukherjee and Peter Caravan*

A. A. Martinos Center for Biomedical Imaging, Massachusetts General Hospital,

Harvard Medical School, 149 13th Street, Suite 2301, Charlestown,

Massachusetts 02129, USA

Email: caravan@nmr.mgh.harvard.edu

Experimental

Materials and Instrumentation. All chemicals and solvents were purchased commercially and used without further purification. NMR spectra were recorded on either 500 MHz or 400 MHz Varian spectrometers. Chemical shifts are reported in δ (ppm). For ^1H and ^{13}C NMR spectra, the residual solvent peaks were used as internal reference, except for the ^{13}C NMR of the ligand where tert-butanol was used as the internal reference.

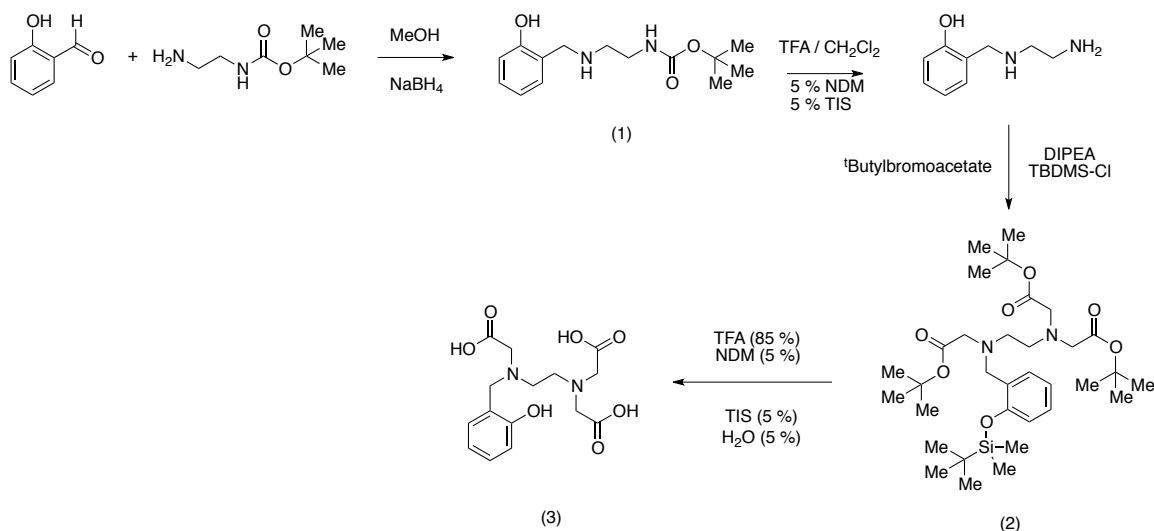
Liquid chromatography-electrospray mass spectrometry (LC-MS) was performed using an Agilent 1100 Series apparatus with an LC/MSD trap and Daly conversion dynode detector with UV detection at 220, 254 and 280 nm. The methods used on this system are as follows: (a) Luna C18 column (100 x 2 mm); eluent A: $\text{H}_2\text{O}/0.1\%$ formic acid, B: MeCN/ 0.1% formic acid; gradient: 5% B to 95% B over 9 minutes; flow rate 0.8 mL/min (used for characterization of organic compounds), and (b) Kromasil C18 column (250 x 4.6 mm); eluent C: 95% MeCN/ 5% 10 mM ammonium acetate, D: 10 mM ammonium acetate; gradient 5% C to 8% C over 14 minutes; flow rate 0.8 ml/min (used for characterization of manganese complexes). Reversed-phase semipreparative purification was performed on a Rainin Dynamax HPLC system with UV detection at 254 nm using a Polaris C18 column. The method used for purification is as follows: The mobile phase A was 50 mM ammonium acetate buffer, pH 6.5 and mobile phase B was a mixture of 5% 50 mM ammonium acetate buffer, pH 6.5/ 95% MeCN. Starting from 5% B, the fraction of B increased to 8% over 23 minutes. The

column was washed with 100% B for 2 minutes and then ramped to 5% B. The system was re-equilibrated at 5% B for 3 minutes.

Relaxivity measurements were performed on a Bruker mq60 Minispec at 1.4 T and 37 °C. Manganese concentrations were determined using an Agilent 7500a ICP-MS system. All samples were diluted with 0.1% Triton X-100 in 5% nitric acid containing 20 ppb of Lu (as internal standard). The ratio of Mn (54.94)/Lu (174.97) was used to quantify the manganese concentration. A linear calibration curve ranging from 0.1 ppb to 200 ppb was generated daily for the quantification. UV-Vis spectra were recorded on a SpectraMax M2 spectrophotometer using quartz cuvette with a 1 cm path length.

Cyclic voltammetry of Mn^{II}HBET, Mn^{II}EDTA and Mn^{III}HBET was recorded using a Nuvant EZstat pro potentiostat in TRIS buffer (pH = 7.4), containing 0.5M KNO₃ as supporting electrolyte, at 100 mVs⁻¹ scan rate. Glassy carbon was used as the working electrode, Ag/AgCl served as the reference electrode and Pt wire was used as the auxiliary electrode. The K₄FeCN₆/K₃FeCN₆ couple was used as the internal standard.

Synthesis



Scheme S1. Complete synthesis of 2'-((2-((carboxymethyl)(2-hydroxybenzyl)amino)ethyl)azanediyl)diacetic acid (HBET) (**3**)

tert-Butyl (2-((2-hydroxybenzyl)amino)ethyl)carbamate (1) : To a solution of salicylaldehyde (12 mmol, 1.465 g) in 90 mL methanol, was added a solution of *tert*-butyl *N*-(2-aminoethyl)carbamate (12 mmol, 1.923 g) in methanol (30 mL) and the solution was stirred for 1 h. To this stirring solution solid NaBH₄ (24 mmol, 0.908 g) was added. Rapid evolution of gas was observed and the solution turned colorless from pale yellow. After stirring for 3 h, all volatiles were removed under reduced pressure, and a white solid was obtained. The residue was dissolved in 200 mL CH₂Cl₂ extracted with 200 mL saturated NaHCO₃ solution. The aqueous layer was extracted with CH₂Cl₂ (2 x 100 mL). All the organics were combined, washed with brine (200 mL) and dried over anhydrous MgSO₄. The solvent was evaporated under reduced pressure to obtain **1** as a pale yellow solid (2.116 g, 97%). ¹H NMR (500 MHz, CDCl₃) δ (ppm): 7.16 (t, *J* = 7.65 Hz, 1H, Ar-*H*), 6.99 (d, *J* = 7.48 Hz, 1H, Ar-*H*), 6.83 (d, *J* = 8.13 Hz, 1H, Ar-*H*), 6.77 (t, *J* = 7.41 Hz, 1H, Ar-*H*), 4.01 (s, 2H, Ar-CH₂N), 3.30 (m, 2H,

NCH₂CH₂N), 2.79 (t, *J* = 5.82 Hz, 2H, NCH₂CH₂N), 1.44 (s, 9H, OC(CH₃)₃).
¹³C{¹H} NMR (100 MHz, CDCl₃) δ (ppm): 157.9 (s, C aromatic), 156.2 (s, NCO₂),
128.5 (s, C aromatic), 128.3 (s, C aromatic), 122.4 (s, C aromatic), 118.9 (s, C
aromatic), 116.1 (s, C aromatic), 79.2 (s, OC(CH₃)₃), 52.1 (s,
ArCH₂NHCH₂CH₂NH), 48.2 (s, ArCH₂NHCH₂CH₂NH), 39.8 (s,
ArCH₂NHCH₂CH₂NH), 28.3 (s, OC(CH₃)₃). Molecular weight for C₁₄H₂₂N₂O₃:
266.34. MS (ESI) *m/z*: Calculated: 267.17 (M+H)⁺; observed: 267.1.

di-*tert*-butyl 2,2'-((2-((2-((*tert*-butoxy)-2-oxoethyl)(2-((*tert*-butyl dimethylsilyl)oxy)-benzyl)amino)ethyl)azanediyl)diacetate (2) : 1 (7.94 mmol, 2.116 g) was dissolved in CH₂Cl₂ (100 mL) followed by addition of 50 mL trifluoroacetic acid. The reaction was stirred for 5 h, and then the volatiles were removed under reduced pressure. The residue was dissolved in water (40 mL) and washed with ether (3 x 40 mL). The water fraction was lyophilized to produce the free amine quantitatively as a white solid, which was used in subsequent reaction without further purification.

The round bottom flask containing the amine was charged with nitrogen, dry CH₂Cl₂ (80 mL) was added and cooled in an ice bath. Under counter argon flow, N, N-diisopropylethylamine (39.70 mmol, 6.91 mL) was added, followed by addition of *tert*-butyldimethylsilyl chloride (8.73 mmol, 1.315 g) as a CH₂Cl₂ solution (10 mL). The solution was allowed to warm to room temperature and stirred for 5 h. The reaction was then cooled to 0 °C and *tert*-butyl bromoacetate (24.61 mmol, 3.63 mL) was added drop wise and the reaction was stirred for 18 h under nitrogen atmosphere. The solution was diluted with CH₂Cl₂ (200 mL) and

washed with saturated NaHCO₃ (3 x 200 mL), brine (1 x 200 mL). All the organics were combined and dried over anhydrous MgSO₄ and evaporated under reduced pressure to obtain a crude yellow oil. The product was purified as colorless oil (1.234 g, 25 %) by using column chromatography (eluent – hexane/ethylacetate, 9:1). ¹H NMR (400 MHz, CDCl₃) δ (ppm): 7.43 (dd, *J*₁ = 1.31 Hz, *J*₂ = 7.57, 1H, Ar-*H*), 7.04 (dt, *J*₁ = 1.71 Hz, *J*₂ = 7.80, 1H, Ar-*H*), 6.88 (t, *J* = 7.51 Hz, 1H, Ar-*H*), 6.72 (d, *J* = 7.93 Hz, 1H, Ar-*H*), 3.76 (s, 2H, Ar-CH₂N), 3.40 (s, 4H, N(CH₂CO₂C(CH₃)₃)₂), 3.29 (s, 2H, N(CH₂CO₂C(CH₃)₃)(CH₂-Ar), 2.81 (m, 4H, NCH₂CH₂N), 1.41 (s, 9H, N(CH₂COC(CH₃)₃)(CH₂-Ar), 1.40 (s, 18H, N(CH₂COC(CH₃)₃)₂), 0.98 (s, 9H, Ar-O-Si(CH₃)₂(C(CH₃)₃), 0.18 (s, 6H, Ar-O-Si(CH₃)₂(C(CH₃)₃)). ¹³C{¹H} NMR (100 MHz, CDCl₃) δ (ppm): 171.1 (s, N(CH₂CO₂C(CH₃)₃)₂), 170.7 (s, N(CH₂CO₂C(CH₃)₃)(CH₂-Ar), 153.7 (s, C aromatic), 130.1 (s, C aromatic), 129.8 (s, C aromatic), 127.4 (s, C aromatic), 121.1 (s, C aromatic), 118.4 (s, C aromatic), 80.6 (s, N(CH₂CO₂C(CH₃)₃)₂), 80.4 (s, N(CH₂CO₂C(CH₃)₃)(CH₂-Ar), 56.1 (s, N(CH₂CO₂C(CH₃)₃)₂), 55.9 (s, N(CH₂CO₂C(CH₃)₃)(CH₂-Ar), 52.8 (s, NCH₂Ar), 52.4 (s, NCH₂CH₂N), 28.2 (s, Ar-CH₂)(CH₂CO₂C(CH₃)₃)NCH₂CH₂N(CH₂CO₂C(CH₃)₃)₂, 25.9 (s, Ar-OSi(CH₃)₂C(CH₃)₃), 18.3 (s, Ar-OSi(CH₃)₂C(CH₃)₃), 4.1 (s, Ar-OSi(CH₃)₂C(CH₃)₃). Molecular weight for C₃₃H₅₈N₂O₇Si: 622.91. MS (ESI) m/z: Calculated: 623.41 (M+H)⁺; observed: 623.4.

2, 2'-((2-((carboxymethyl)(2-hydroxybenzyl)amino)ethyl)azanediyl)diacetic acid (HBET) (3) : **2** (1.98 mmol, 1.234 g) was dissolved in trifluoroacetic acid (40 mL) followed by addition of triisopropylsilane (2.35 mL), 1-dodecanethiol (2.35

mL) and water (2.35 mL). The reaction was stirred for 5 h, and then the volatiles were removed under reduced pressure. The residue was dissolved in water (40 mL) and washed with ether (3 x 40 mL). The water fraction was lyophilized to produce **3** quantitatively as a white solid. ^1H NMR (500 MHz, D_2O) δ (ppm): 7.44 (m, 2H, Ar-H), 7.03 (m, 2H, Ar-H), 4.57 (s, 2H, Ar- CH_2N), 4.04 (s, 2H N($\text{CH}_2\text{CO}_2\text{H}$)($\text{CH}_2\text{-Ar}$), 3.66 (s, 4H, N($\text{CH}_2\text{CO}_2\text{H}$) $_2$), 3.54 (t, $J = 6.09$, 2H, N $\text{CH}_2\text{CH}_2\text{N}$), 3.35 (t, $J = 5.9$ Hz, 2H, N $\text{CH}_2\text{CH}_2\text{N}$). $^{13}\text{C}\{^1\text{H}\}$ NMR (125 MHz, D_2O) δ (ppm): 174.1 (s, N($\text{CH}_2\text{CO}_2\text{H}$) $_2$), 169.9 (s, N($\text{CH}_2\text{CO}_2\text{H}$)($\text{CH}_2\text{-Ar}$), 156.3 (s, C aromatic), 133.6 (s, C aromatic), 133.0 (s, C aromatic), 121.5 (s, C aromatic), 116.6 (s, C aromatic), 116.3 (s, C aromatic), 55.6 (s, (HO_2CCH_2) $_2\text{NCH}_2\text{CH}_2\text{N}(\text{CH}_2\text{CO}_2\text{H})(\text{CH}_2\text{-Ar}$), 54.8 (s, N CH_2Ar), 52.0 (s, N $\text{CH}_2\text{CH}_2\text{N}$), 49.9 (s, N $\text{CH}_2\text{CH}_2\text{N}$). Molecular weight for $\text{C}_{15}\text{H}_{20}\text{N}_2\text{O}_7$: 340.33. MS (ESI) m/z : Calculated: 341.13 (M+H) $^+$; observed: 341.1.

$\text{Na}_2[\text{Mn}^{\text{II}}\text{HBET}]$ (4) : 3 (0.26 mmol, 0.089 g) was dissolved in 5 mL water. The pH was adjusted to 8 using 1 N sodium hydroxide solution. $\text{MnCl}_2 \cdot 4\text{H}_2\text{O}$ (0.26 mmol, 0.051 g) was then added to the solution and the pH was carefully adjusted to 5. The reaction was stirred for 1 h, filtered and lyophilized to yield a white solid. The complex was injected onto a reverse phase C18 (Polaris) column and desalted using the method described above. Fractions were collected and lyophilized to yield **4** as a white solid (0.095 g, 84%). Molecular Weight for $\text{C}_{15}\text{H}_{18}\text{MnN}_2\text{O}_7$: 393.25. MS (ESI) m/z : Calculated: 394.26 (M+H) $^+$; Observed: 394.1.

$\text{Na}[\text{Mn}^{\text{III}}\text{HBET}]$ (5) : 3 (0.15 mmol, 0.05 g) was dissolved in 5 mL water. The pH was adjusted to 8 using 1 N sodium hydroxide solution. $\text{MnCl}_2 \cdot 4\text{H}_2\text{O}$ (0.15 mmol,

0.030 g) was then added to the solution and the pH was adjusted to 12. The solution was allowed to stir for 1 h. The solution was then filtered through a 0.45 μm filter to remove MnO_2 , pH adjusted to 11 and the solution was stirred for 18 h. The reaction was followed using analytical LC-MS and the reaction was stopped when 70% conversion to the Mn^{III} species was observed. The mixture was purified by prep-HPLC as described above. The fractions were collected and lyophilized to yield **5** as a brown solid (0.023 g, 38%). Molecular Weight for $\text{C}_{15}\text{H}_{17}\text{MnN}_2\text{O}_7$: 392.24. MS (ESI) m/z : Calculated: 393.25 ($\text{M}+\text{H}$)⁺; Observed: 393.1.

Na[Mn^{III}HBED] (6) : 2,2'-(ethane-1,2-diylbis((2-hydroxybenzyl)azanediyl))dicaetic acid (HBED) (0.15 mmol, 0.0641 g) was dissolved in 4 mL water. The pH was adjusted to 8 using 1 N sodium hydroxide solution. $\text{MnCl}_2 \cdot 4\text{H}_2\text{O}$ (0.15 mmol, 0.030 g) was then added to the solution and the pH was adjusted to 12. The solution was allowed to stir for 1 h. The solution was then filtered through a 0.45 μm filter to remove MnO_2 , and the pH was then adjusted to 11 and the solution was stirred for 18 h. The reaction was followed using analytical LC-MS and showed the formation of clean Mn^{III} HBED species at the end of 18 h. The complex was injected onto a reverse phase C18 (Polaris) column and desalted using the method described above. The fractions were collected and lyophilized to yield **6** as a deep brown solid (0.052 g, 74%). Molecular Weight for $\text{C}_{20}\text{H}_{21}\text{MnN}_2\text{O}_6$: 440.33. MS (ESI) m/z : Calculated: 441.33 ($\text{M}+\text{H}$)⁺; Observed: 441.1.

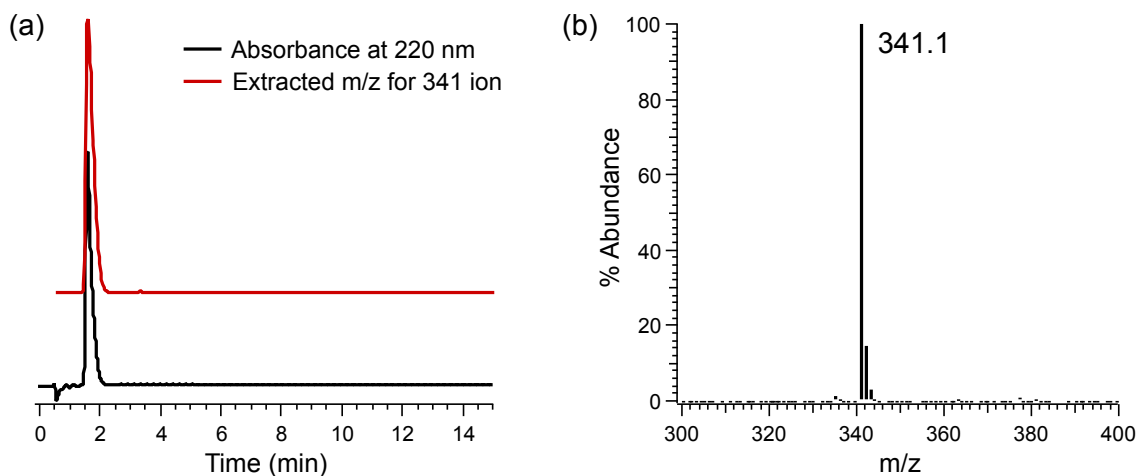


Figure S1. (a) Analytical LC-MS traces of ligand HBET (**3**) where the trace at 220 nm (black line) indicates the high purity of the sample and the extracted ion for $m/z = 341$ is shown in red line which overlaps with the above trace and (b) ESI-MS of **3** displaying the $m/z = 341$ corresponding to the $[M+H]^+$.

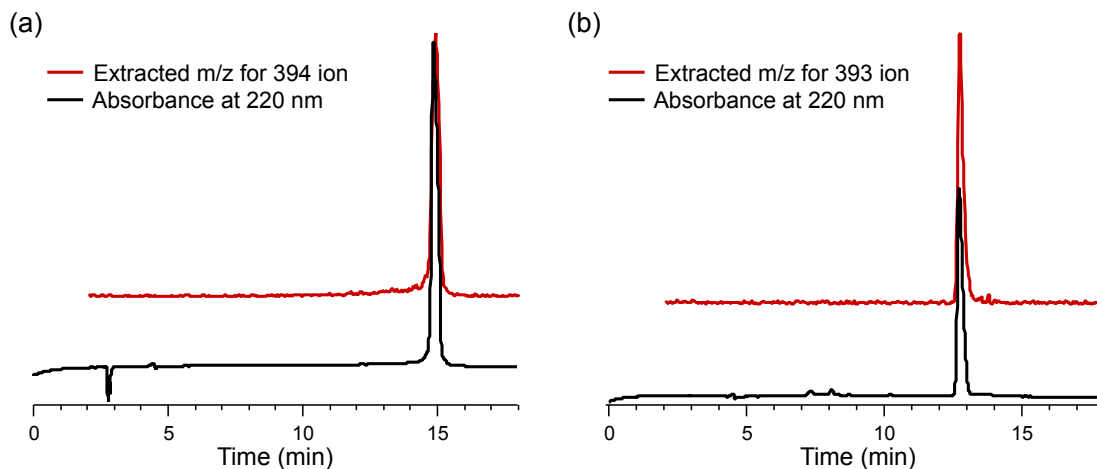


Figure S2. Analytical LC-MS traces of (a) Mn^{II}HBET (**4**) and (b) Mn^{III}HBET (**5**) on a C18 reversed-phase column; where the trace at 220 nm (black line) indicates the high purity of the sample and the extracted ion for $m/z = 394$ and 393 is shown in red line.

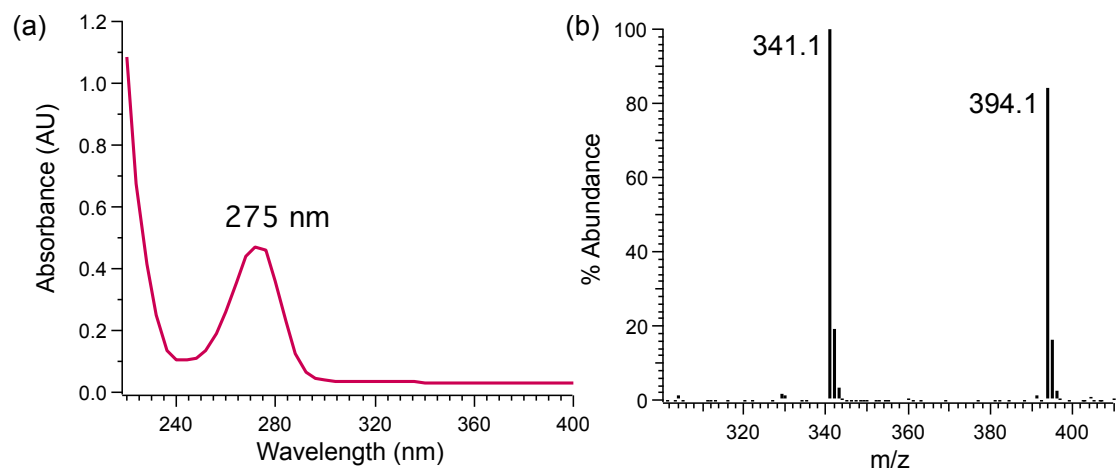


Figure S3. (a) UV spectrum of Mn^{II}HBET (**4**) in water. (b) ESI-MS of Mn^{II}HBET (**4**) displaying m/z = 394 corresponding to [M+H]⁺.

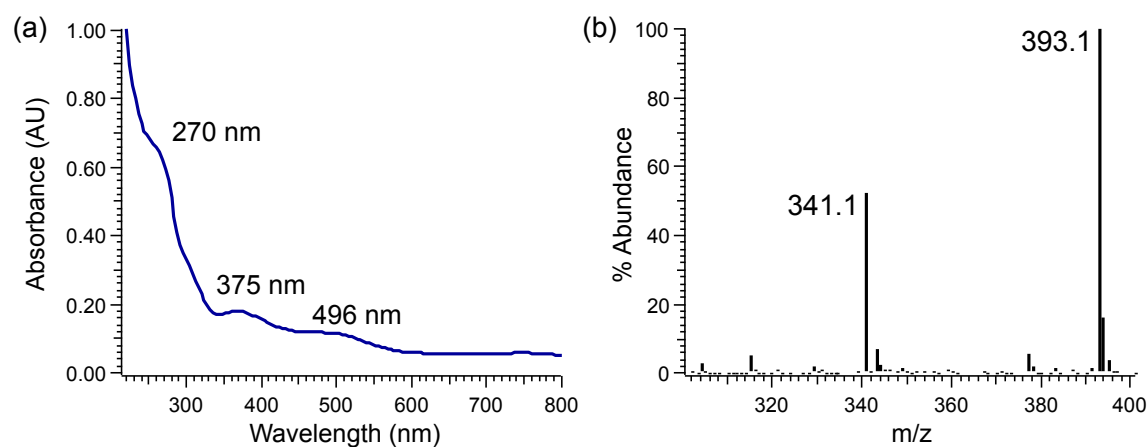


Figure S4. (a) UV spectrum of Mn^{III}HBET (**5**) in water. (b) ESI-MS of Mn^{III}HBET (**5**) displaying m/z = 393 corresponding to [M+H]⁺.

Relaxometric Study. T_1 was measured with an inversion recovery pulse sequence taking 10 inversion times. Relaxivity was determined from the slope of a plot of $1/T_1$ vs concentration of Na₂[Mn^{II}HBET] (**4**) and Na[Mn^{III}HBET] (**5**) in TRIS buffer, pH = 7.4 at 37 °C. The concentration of manganese in each stock solution was determined using ICP-MS.

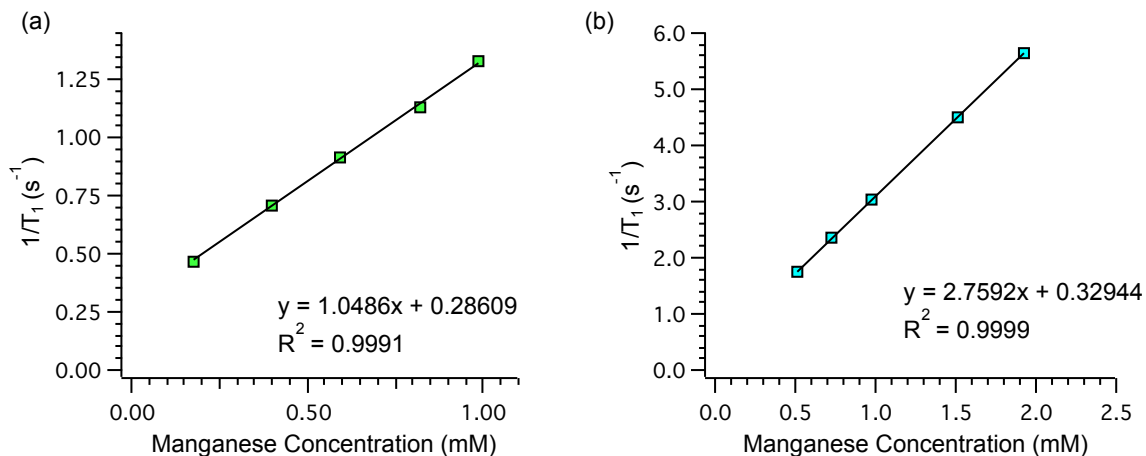


Figure S5. Relaxivity of (a) $\text{Na}[\text{Mn}^{\text{III}}\text{HBET}]$ (**5**) and (b) $\text{Na}_2[\text{Mn}^{\text{II}}\text{HBET}]$ (**4**) in TRIS buffer. $1/T_1$ vs $[\text{Mn}]$ for **4** and **5** measured in TRIS buffer at pH 7.4, 37 °C. The slope of the line gives the relaxivity.

Electrochemistry.

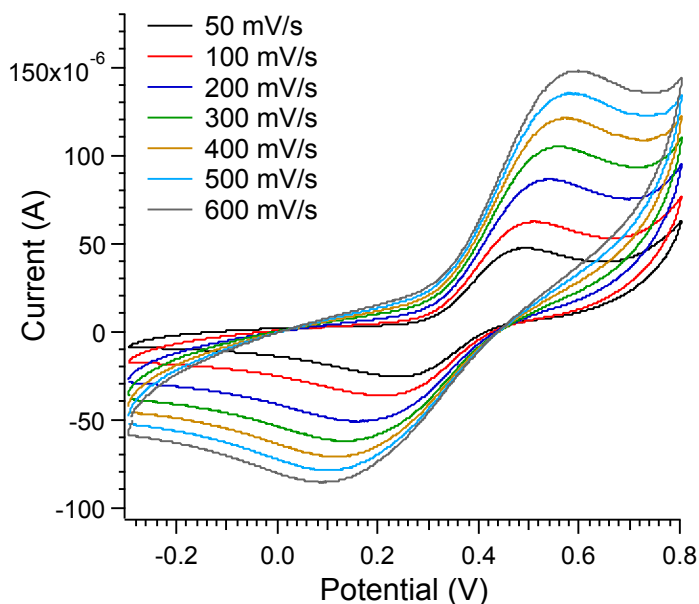


Figure S6. Cyclic voltammogram of $\text{Mn}^{\text{II}}\text{HBET}$ (25 mM) in TRIS buffer (pH = 7.4) containing KNO_3 as the supporting electrolyte at different scan rates ranging from 50 – 600 mV/s.

Kinetic Experiments for the Reduction Reaction.

This series of kinetic experiments were conducted at 37° C (pH 7.4) to determine the empirical rate law for the reduction of Mn^{III}-HBET by glutathione. The Mn^{III}-HBET complex possesses a strong absorbance band at 375 nm ($\epsilon = 1.38 \times 10^3 \text{ M}^{-1} \text{ cm}^{-1}$) in water that is not present in the UV spectrum of the Mn^{II}-HBET complex. This feature was used to monitor the reduction of Mn^{III}-HBET over time. Initial reaction rates were measured at a three different GSH concentrations (5 mM, 10 mM and 20 mM). Additionally, for each GSH concentration, the reaction was performed at four different initial concentrations of Mn^{III}-HBET (0.3 mM, 0.4 mM, 0.5 mM and 0.6 mM). By using a large excess of GSH in these experiments, we found the reaction behaved pseudo first-order with respect to the Mn^{III}-HBET complex as expressed in equation S1.

$$\left[\text{Mn}^{\text{III}} \text{HBET} \right]_t = \left[\text{Mn}^{\text{III}} \text{HBET} \right]_o \cdot e^{-k_{\text{obs}} \cdot t} \quad \text{eq. S1}$$

Here, the observed rate constant (k_{obs}) is simply the product of the actual rate constant (k) and [GSH], t is time, and the subscripts 't' and 'o' refer to the concentration at time 't' or the initial concentration, respectively. Supplemental Figure S8 shows two sets of kinetic experiments in which we have plotted the natural log of $[\text{Mn}^{\text{III}}\text{-HBET}]_t$ as a function of time. In this way, the slope of each line is equal to $-k \cdot [\text{GSH}]$ and the intercept is $\ln[\text{Mn}^{\text{III}}\text{-HBET}]_o$. Based on these experiments, we determined that the reaction was first-order in both [GSH] and $[\text{Mn}^{\text{III}}\text{-HBET}]$ with an overall second-order rate constant of $(3.8 \pm 0.3) \times 10^{-1} \text{ M}^{-1} \text{ s}^{-1}$.

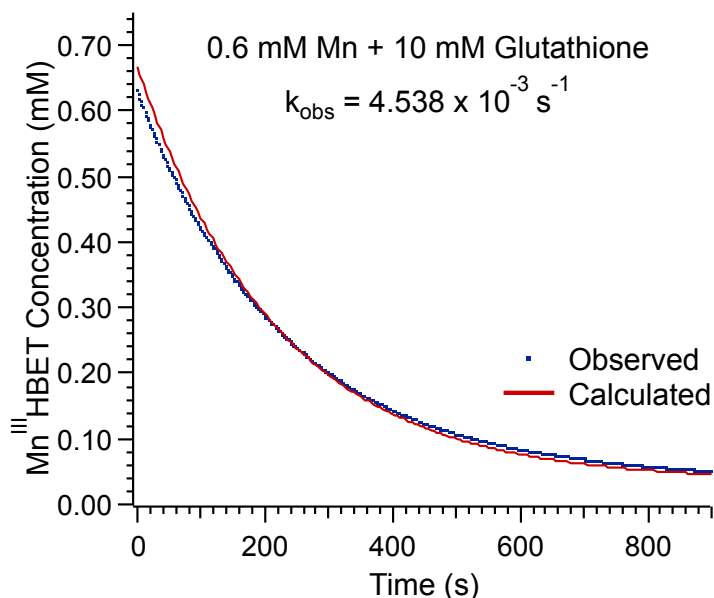


Figure S7. Conversion of Mn^{III} -HBET to Mn^{II} -HBET in the presence of glutathione as measured by the decrease of the absorbance at 375 nm (dotted line). The solid line shows the fitting of the observed data to a first order rate equation with respect to Mn^{III} under pseudo first order conditions (equation S1).

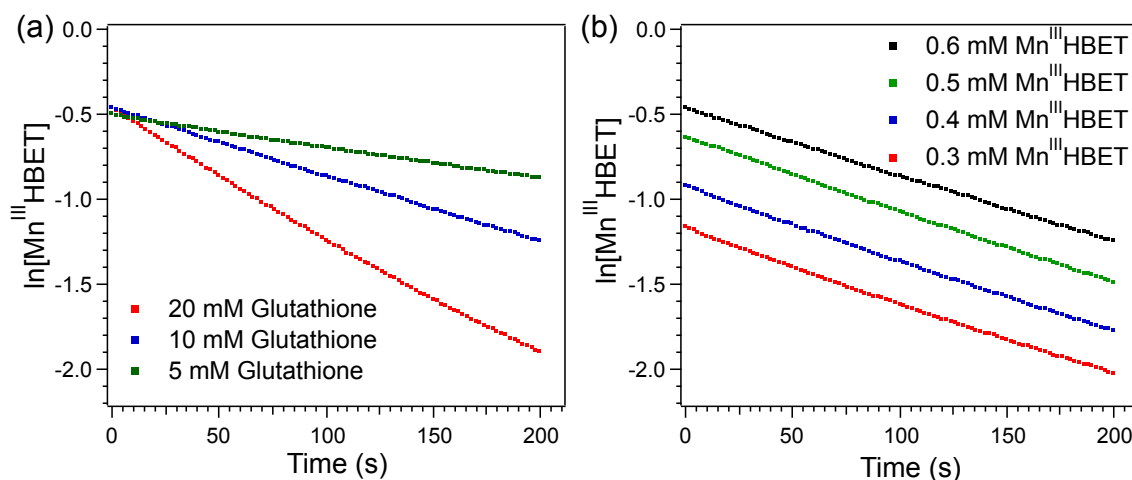


Figure S8. In the presence of a large excess of reduced glutathione the redox reaction behaves pseudo first order with respect to $[\text{Mn}^{\text{III}}\text{-HBET}]$. The slope of each line is equal to $-k \cdot [\text{GSH}]$ (see equation S1). a.) The concentration of glutathione is varied in each reaction while the initial concentration Mn^{III} -HBET (0.6 mM) is not. b.) The initial Mn^{III} -HBET concentration is varied while the glutathione concentration (10 mM) is held constant.

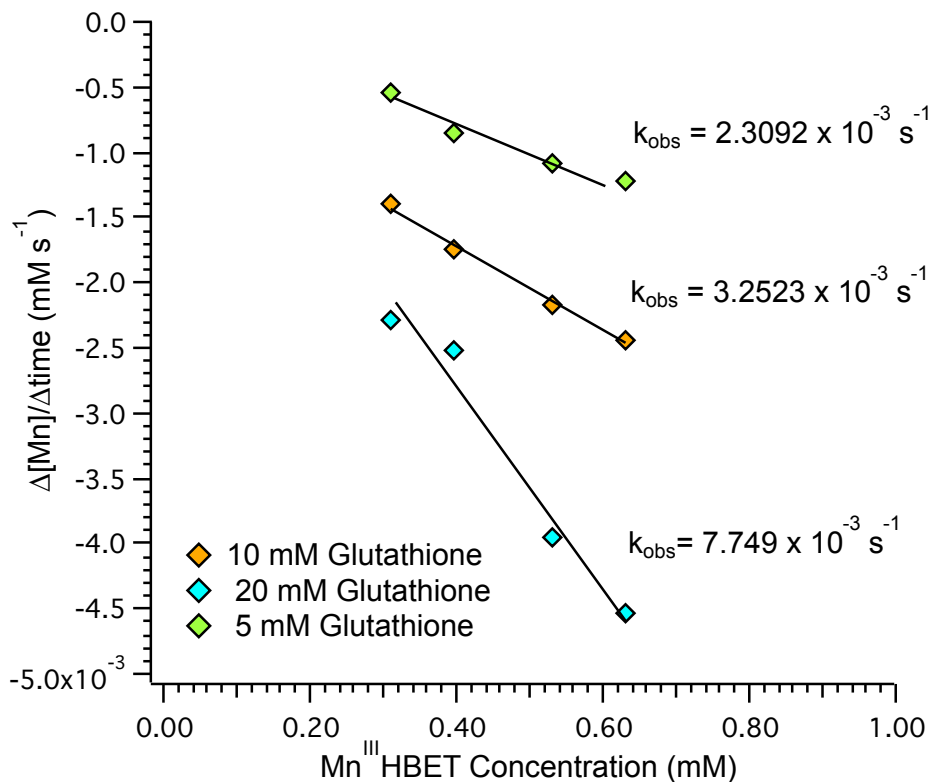
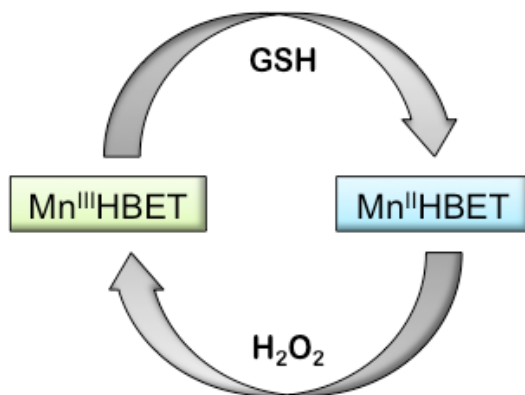


Figure S9. Plot of initial rate for Mn^{III}HBET reduction as a function Mn^{III}HBET concentration at three different glutathione concentrations. The slope of each line (k_{obs}) is equal to $-k \cdot [GSH]$ (see equation S1).

Oxidation of Mn^{II}HBET with hydrogen peroxide.



Scheme S2. Interconversion between the two oxidation states with reducing agent (GSH) and oxidizing agent (H₂O₂).

The oxidation of $\text{Mn}^{\text{II}}\text{HBET}$ with H_2O_2 (1 mM) in TRIS buffer (pH = 7.4) was followed using UV-Vis spectroscopy, relaxivity measurements, and LC-MS. Unlike the reduction of $\text{Mn}^{\text{III}}\text{HBET}$ with glutathione, the oxidation reaction appears to reach equilibrium after 70% conversion to $\text{Mn}^{\text{III}}\text{HBET}$ as calculated from LC-MS data.

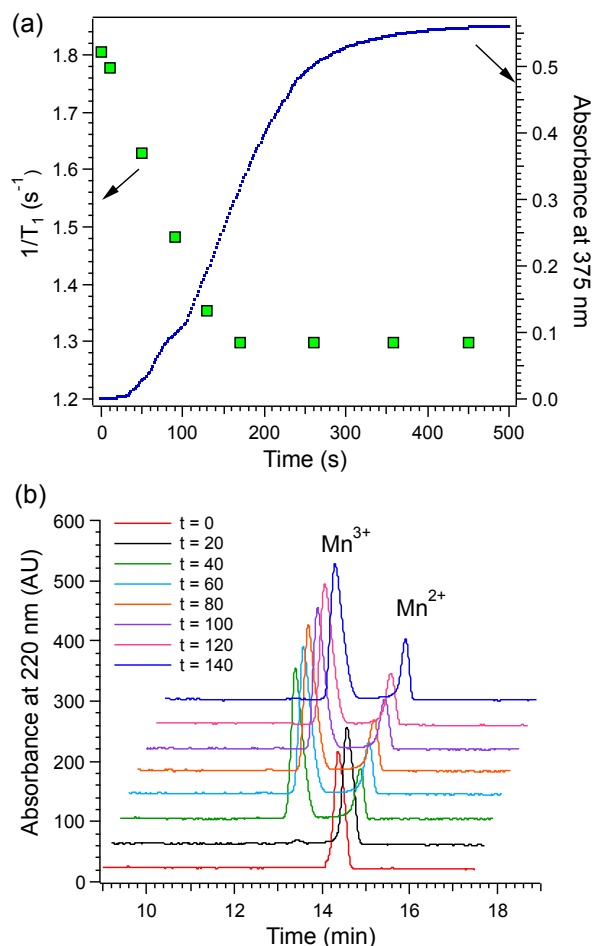


Figure S10. (a) Oxidation of 0.5 mM $\text{Mn}^{\text{II}}\text{-HBET}$ to $\text{Mn}^{\text{III}}\text{-HBET}$ with 1 mM H_2O_2 in TRIS buffer (pH 7.4, 37 °C) followed by relaxivity measurements (left axis) and UV-Vis spectroscopy, where the increase in the UV absorbance at 375 nm indicates the formation of $\text{Mn}^{\text{III}}\text{HBET}$ as a function of time (right axis). (b) Oxidation of 0.5 mM $\text{Mn}^{\text{II}}\text{-HBET}$ by 1 mM H_2O_2 at 26 °C monitored by LC-MS.

MR Imaging. MR imaging was performed using a Bruker Biospec 4.7T system. Three samples (~500 μL) were placed in a homemade sample holder and imaged using a volume coil. Acquisition matrix = 64×256 for $0.234 \times 0.312 \text{ mm}^2$ in-plane resolution; slice thickness = 5 mm. T_1 -weighted images were obtained with a fast low angle shot (FLASH) gradient echo sequence: TR/TE/FA = 20/5.44/40° with 8 averages. T_1 was determined using a 2D rapid acquisition refocused echo (RARE) inversion recovery sequence: TR = 3200 ms, TE = 9.7 ms. Inversion times (TI): 5, 45, 85, 165, 325, 645, 1285, 1925 and 3205 ms. T_1 was obtained from a nonlinear least square fit of the signal intensity (SI(t)) vs TI curve where T_1 , SI(0) and a are adjustable parameters, equation S1.

$$SI(t) = SI(0)[1 - a \cdot e^{TI/T_1}] \quad (S1)$$

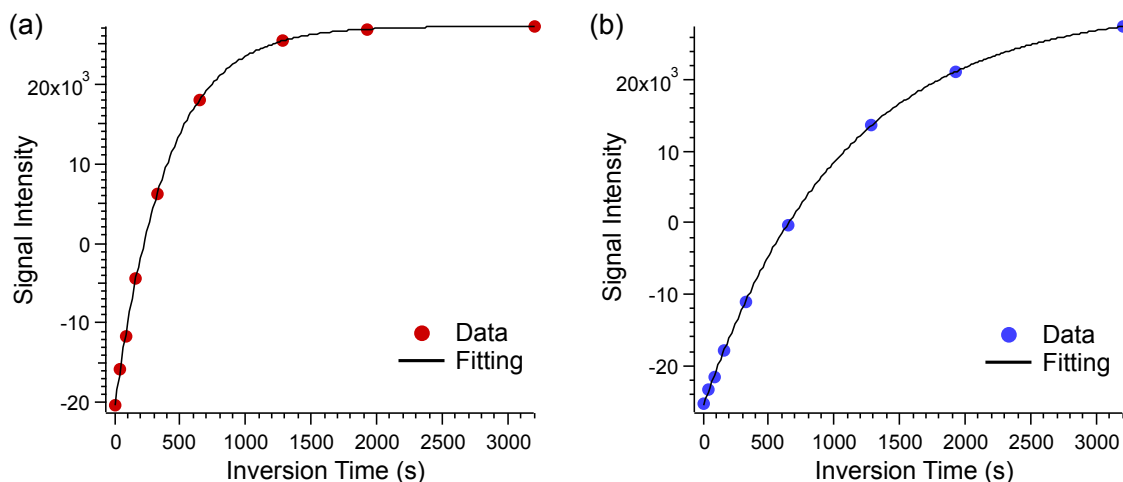


Figure S11. Representative plots of signal intensity vs inversion time (TI) for (a) 0.5 mM Mn^{II} -HBET and (b) 0.5 mM Mn^{III} -HBET in TRIS buffer (pH = 7.4). Note the faster signal recovery for Mn^{II} -HBET indicating a shorter T_1 and higher relaxivity than Mn^{III} -HBET.

Stability of Mn^{II}HBET and Mn^{III}HBET complexes

The stability of the manganese complexes were measured in different buffers using concentrations similar to those found in the blood plasma (1mM phosphate buffer, 25 mM sodium bicarbonate buffer and 0.1 mM citrate buffer). A solution, 0.5 mM, of the manganese complex was incubated in the respective buffers at 37 °C (pH = 7.4) and the species were then quantified on the LC-MS using the method as described earlier. The manganese complexes (0.5 mM) were also treated with EDTA (0.5 mM) in TRIS buffer (pH = 7.4) and incubated at 37 °C for 1h. The species were then quantified on the LC-MS using the method as described earlier.